SUPPLEMENTARY MATERIAL

Synergy Effect Between Photocatalysis and Heterogeneous PhotoFenton Catalysis on Ti-Doped $LaFeO_3$ Perovskite for High Efficiency Light-Assisted Water Treatment

Patricia Garcia-Muñoz,,† Fernando Fresno, ‡ Christophe Lefevre, ⁑ Didier Robert, † and Nicolas Keller*,†*

† Institut de Chimie et Procédés pour l'Energie, l'Environnement et la Santé (ICPEES) CNRS/University of Strasbourg, 25 rue Becquerel, Strasbourg, France

‡ Photoactivated Processes Unit, IMDEA Energy Institute. Avda. Ramón de la Sagra, 3, Parque Tecnológico de Móstoles, 28935 Móstoles (Madrid), Spain

⁑ Institut de Physique et de Chimie des Matériaux de Strasbourg (IPCMS), CNRS/University de Strasbourg, 23 rue du Loess, Strasbourg, France

Table S1. Refined crystallographic data of the LFO, P25-LFO and SG-LFO samples

		La		O1			O2	
	a,b,c (Å)	x	y	x	y	z	x	y
LFO	5.547(1) 5.560(1) 7.861(1)	0.995(1)	0.0271(5)	0.72(1)	0.279(7)	0.045(5)	0.06(1)	0.491(5)
P25-LFO	5.525(1) 5.553(1) 7.860(1)	0.002(2)	0.018(1)	0.74(1)	0.266(8)	0.052(3)	0.02(3)	0.466(7)
SG-LFO	5.526(1) 5.554(1) 7.854(1)	0.001(2)	0.016(1)	0.77(1)	0.224(9)	0.050(4)	0.03(3)	0.502(6)

Table S2. Refined crystallographic data of the SG-LFO#1SG-LFO#3 and SG-LFO#5 samples corresponding to the SG-LFO sample after 1st, 3rd and 5th test.

		La		O1			O2	
	a,b,c (Å)	x	y	x	y	z	x	y
SG-LFO#1	5.526(1) 5.554(1) 7.854(1)	0.001(2)	0.016(1)	0.77(1)	0.224(9)	0.050(4)	0.03(3)	0.502(6)
SG-LFO#3	5.525(1) 5.555(1) 7.853(1)	0.003(3)	0.016(1)	0.76(1)	0.224(9)	0.047(3)	0.02(3)	0.505(6)
SG-LFO#5	5.527(1) 5.551(2) 7.853(1)	0.003(3)	0.009(3)	0.71(2)	0.224(10)	0.054(6)	0.03(2)	0.519(12)

Figure S1. SEM images of the (A-B) LFO, (C-D) P25-LFO and (E-F) SG-LFO catalysts.

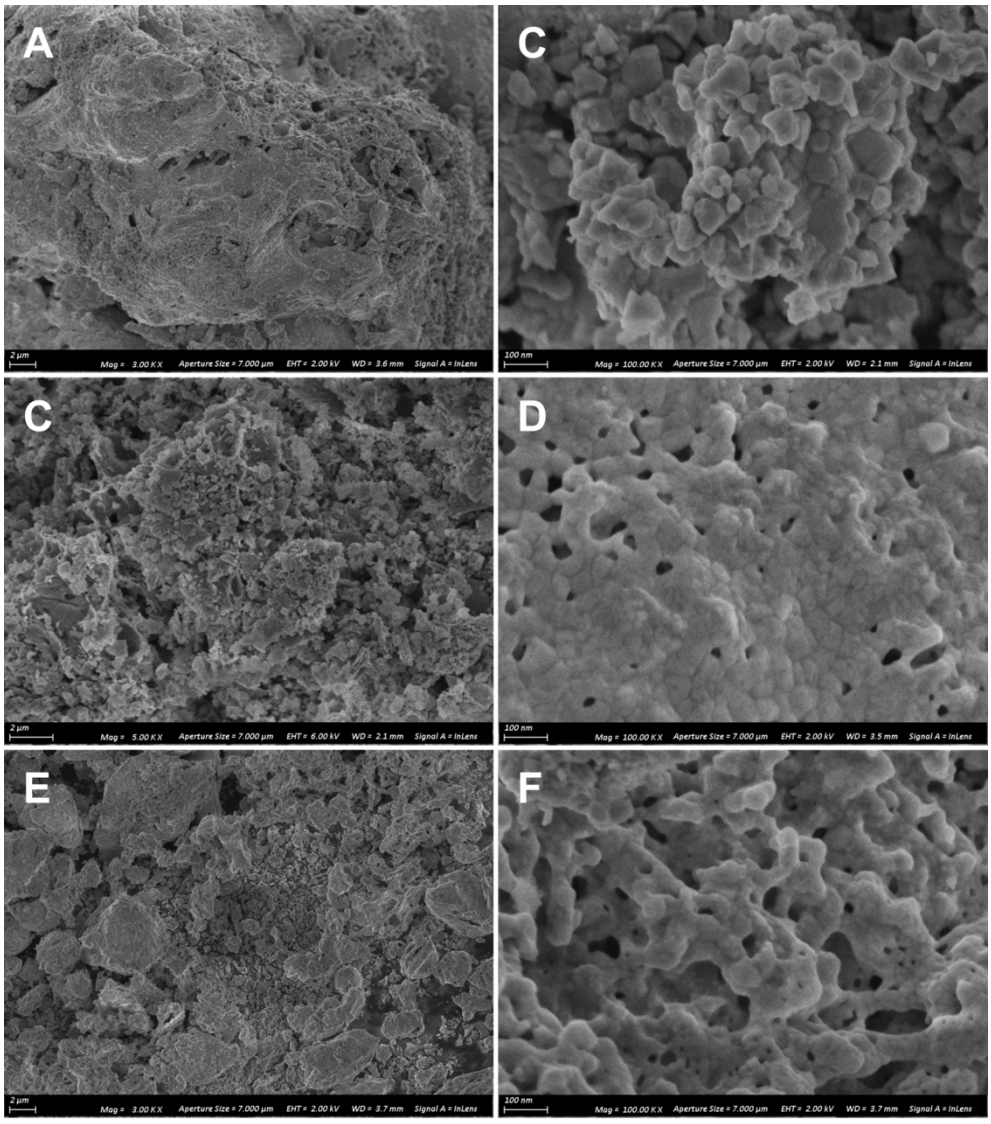

Figure S2. TEM images of the pristine LFO catalyst. The interplanar distances of 0.39 nm, 0.28 nm and 0.23 nm corresponded to the (110), (100) and (111) planes of the LFO structure, respectively.

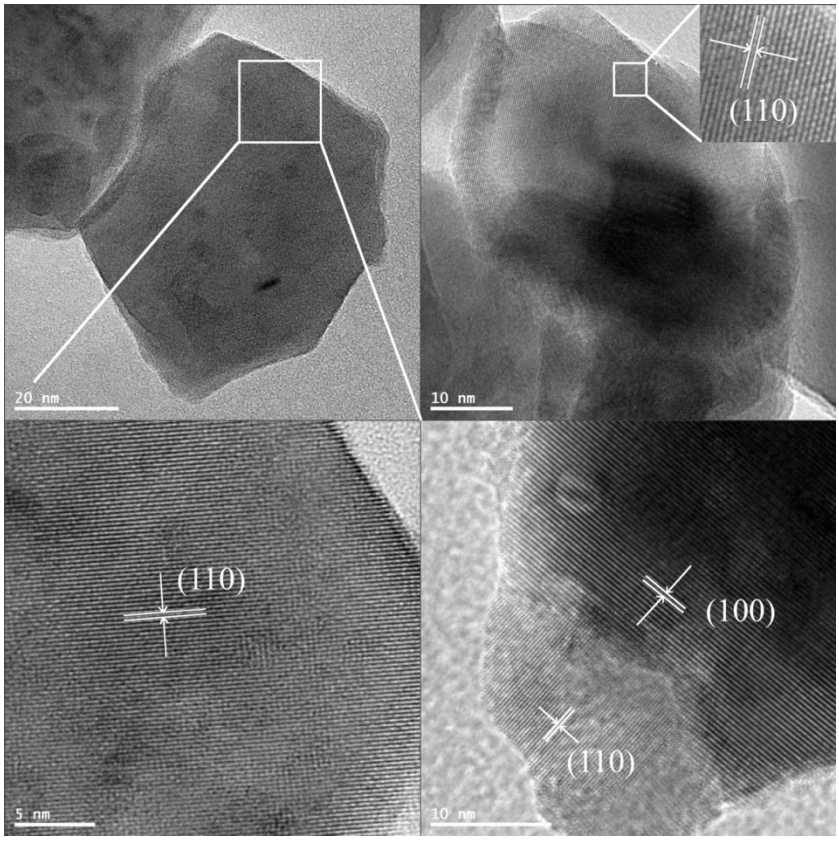

Figure S3. UPS spectra recorded on the pristine LFO and the Ti-substituted SG-LFO catalysts (He I, $h\lambda$ = 21.2 eV), allowing the graphical determination of the valence band maximum (VBM).

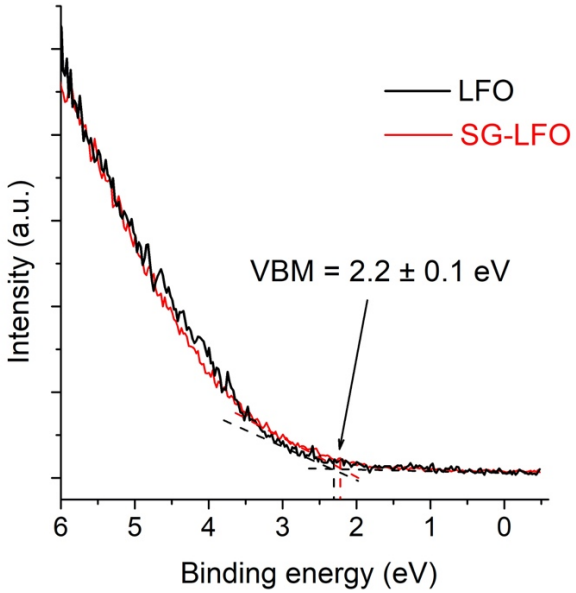

The value of the valence band maximum (VBM) has been determined as usually by fitting a straight line onto the leading edge. Taking into account the accuracy of the measurement on nanocrystalline powders, the Ti → La partial substitution did not result in any significative change in the VBM that has been determined graphically at *ca.* 2.2 ± 0.1 eV *vs.* Fermi level, whether the surface is modified or not by titanium.

Combined with UV-vis DRS that revealed that the band-gap was not influenced by the partial substitution (at *ca.* 2.1 eV), UPS data showed that the energy position of the conduction band was not significantly modified and remained close to the Fermi level.

Similar values have been reported for $LaFeO_3$, whether they have been obtained by rough calculation according to the Mulliken electronegativity theory (J. Yang et al., *Chem. Commun.*, 52 (2016) 2620 ; C. Gong et al. *New J. Chem., 43 (*2019) 16506) or though UPS analysis (J. E. Kleibeuker et al., Physical Review Letters, 113 (2014) 237402).

Figure S4. Observed (black), calculated (red full line), and difference (blue full line) x-ray powder diffraction patterns of (a) SG-LFO#1 (b) SG-LFO#3 and (c) SG-LFO#5 catalysts recorded on a D8 diffractometer (λ = 1.54056 Å). Positions of the Bragg reflections are represented by vertical bars, in blue for the reflexes indexed in the Pbnm orthorhombic unit cell of $LaFeO_3$ and in green for those of the α-Fe_2O_3 extra phase.